Ecotoxicology and Environmental Safety 302 (2025) 118707

Contents lists available at ScienceDirect

Ecotoxicology and Environmental Safety

journal homepage: www.elsevier.com/locate/ecoenv

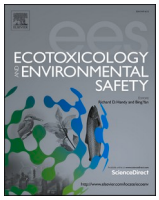

Study on toxicity and bioavailability of metals from urban $PM_{2.5}$ and PM_{10} extracted in simulated biological fluids: *in vitro* and *in vivo* assessment

Juri Rimauro [a], Gaetana Napolitano [b], Gianluca Fasciolo [c], Paola Venditti [c], Angelo Riccio [b,*], Elena Chianese [b,*]

[a] Italian National Agency for New Technologies, Energy and Sustenaible Economic Development (ENEA), Portici Research Centre, Piazzale E. Fermi 1, Portici 80055, Italy
[b] Department of Science and Technology, Parthenope University of Naples, Centro Direzionale Isola C4, Naples 8143, Italy
[c] Department of Biology, University of Naples Federico II, Complesso Monte Sant'Angelo Via Cintia 26, Napoli 80126, Italy

ARTICLE INFO

Keywords:
Particulate matter
Metals
Simulated biological fluids
Toxicity
Artemia franciscana
Oxidative stress

ABSTRACT

Airborne particulate matter (PM), particularly fine ($PM_{2.5}$) and coarse (PM_{10}) fractions, contains toxic metals that contribute to oxidative stress development and adverse health effects. This study evaluates the bioavailability and toxicity of both regulated metals (Pb, Cd, Ni, As) and unregulated metals (Fe, Cu, Zn, V) in urban PM using simulated biological fluids (SBFs) to replicate different human exposure routes. The metal solubility was assessed using Gamble's solution (neutral lung interstitial fluid), artificial lysosomal fluid (ALF), artificial saliva, and artificial tear fluid, simulating inhalation, ingestion, and ocular contact, respectively. Results indicate that acidic fluids (ALF) significantly increased the solubility of Cu, Pb, and Fe, particularly in $PM_{2.5}$, due to enhanced proton-driven metal leaching. $PM_{2.5}$ extracts consistently exhibited higher bioavailable metal concentrations than PM_{10}, reflecting the greater surface area and reactivity of fine particles. Toxicological evaluations using the *Artemia franciscana* model revealed that PM exposure alters redox homeostasis by increasing reactive oxygen species (ROS) content, lipid peroxidation, and protein carbonylation and inducing the increase in antioxidant activity of the enzymes glutathione peroxidase and reductase. $PM_{2.5}$ extracts had a greater toxic impact, suggesting a stronger link between fine particulate-bound metals and oxidative damage. By standardizing SBFs and integrating information obtained through chemical and biological approaches we get more information on the bioavailability and potential harmful effects of metals associated with PM. The findings highlight the need for more stringent air quality controls, mainly targeting $PM_{2.5}$ due to its increased metal bioavailability and toxicity. Furthermore, this study validates *Artemia franciscana* as a cost-effective and ethically acceptable model for *in vivo* toxicological assessments.

1. Introduction

Particulate matter (PM) has emerged as a critical concern in environmental health due to its well-documented impacts on human health and ecological systems (Peters, 2005; Valavanidis et al., 2008; Pelucchi et al., 2009; Li and Gao, 2014; Kim et al., 2015; Nemmar et al., 2004). PM, particularly fine particles ($PM_{2.5}$) and coarse particles (PM_{10}) contains a diverse array of chemical components, including transition metals, polycyclic aromatic hydrocarbons (PAHs), organic compounds, and biological materials (Ali et al., 2019; EzhilKumar et al., 2021). Among these constituents, metals play a crucial role in generating reactive oxygen species (ROS) in biological systems, leading to oxidative stress—a major mechanism underlying PM-induced toxicity (Ercal et al., 2001; Halliwell and Gutteridge, 1990).

Oxidative stress is defined as a state of imbalance between the production of ROS and the capacity of a biological system to counteract the harmful effects of ROS through the antioxidant defense system (Sies, 2018). ROS are all byproducts of normal cellular metabolism (and include highly reactive hydroxyl radicals ($^{\bullet}OH$, $^{\bullet}O_2^-$), and less reactive species like hydrogen peroxide (H_2O_2). When ROS production exceeds the cellular antioxidant capacity, lipid peroxidation, protein oxidation, and DNA damage appear (Napolitano et al., 2022), which can result in chronic inflammation, respiratory diseases, cardiovascular disorders, and even cancer (Khansari et al., 2009).

* Corresponding authors.
E-mail addresses: angelo.riccio@uniparthenope.it (A. Riccio), elena.chianese@uniparthenope.it (E. Chianese).

https://doi.org/10.1016/j.ecoenv.2025.118707
Received 21 March 2025; Received in revised form 30 June 2025; Accepted 16 July 2025
Available online 21 July 2025

The generation of ROS by PM is associated with its specific constituents, particularly transition metals such as iron (Fe), copper (Cu), and vanadium (V), which participate in redox reactions like the Fenton reaction. This process produces highly reactive hydroxyl radicals capable of initiating oxidative damage (Kehrer and Klotz, 2015; Liochev, 2018). Redox-inactive metals, such as lead (Pb) and cadmium (Cd), exacerbate oxidative stress by depleting cellular antioxidants and impairing enzymatic functions (Wu et al., 2016). Furthermore, interactions between PM-associated organics, such as PAHs and quinones, and cellular systems can amplify ROS production through mechanisms like redox cycling (Squadrito et al., 2001). The interplay between these factors underscores the complex mechanisms by which PM induces oxidative damage.

To advance understanding of these mechanisms, recent studies have emphasized the importance of bioavailable metal fractions, which more accurately represent the health risks associated with PM exposure compared to total metal content (Wiseman, 2015; Kastury et al., 2017). Bioavailability is influenced by the composition of biological fluids, making the use of simulated biological fluids (SBFs) essential for assessing the solubility and potential toxicity of PM-bound metals under realistic conditions. Simulated fluids such as Gamble's solution (neutral pH interstitial lung fluid) and artificial lysosomal fluid (acidic pH macrophage environment), provide valuable insights into how metals interact with different biological environments (Wiseman, 2015).

Additionally, the inclusion of other simulated fluids, such as artificial saliva and tear fluid, broadens the scope of investigation to encompass oral and ocular exposure pathways, further improving our understanding of PM bioavailability across different exposure routes (Marques et al., 2011). Recent data, in fact, support a link between PM exposure and the development of ocular pathologies, including dry eyes, conjunctivitis, myopia, glaucoma, and trachoma (Muruganandam et al., 2023). Similarly, saliva plays a crucial role in the ingestion of metals present in PM. A study by Li et al. (2024) examined the interaction between diesel exhaust particulate matter (DEPM) and mucins in simulated saliva. The findings revealed that DEPM binds to salivary mucins, modifying the particles' properties, increasing the release of heavy metals such as chromium (Cr), iron (Fe), and zinc (Zn), and inducing oxidative damage to salivary proteins. Furthermore, research by Sousa et al. (2023) analyzed the metal content in the saliva of firefighters, a class of workers with high exposure to airborne pollutants. The study detected multiple metals, including lead (Pb), cadmium (Cd), and mercury (Hg), in all saliva samples.

However, despite advancements in the SBFs use, several challenges persist. Studies often lack consistency in SBFs composition, particle size relevance, and extraction efficiency (Wiseman, 2015; Kastury et al., 2017). Prior research has been constrained using unrealistic PM concentrations, inadequate representation of physiological conditions, and limited exploration of PM's size-dependent effects (Wiseman, 2015). The diversity in experimental approaches complicates cross-study comparisons, while the absence of standardized protocols hampers reproducibility. Moreover, correlations between *in vitro* and *in vivo* findings remain sparse, limiting biological relevance. For instance, while SBFs simulate respiratory conditions, their predictive power for *in vivo* scenarios is limited without robust validation using animal experimental models (Innes et al., 2021). Therefore, the use of simulated fluids allows us to obtain information on the content of potentially toxic metals from PM, but information on their effective toxicity can be obtained only on biological systems.

Studies conducted in living organisms evaluating cellular biomarkers such as protein-bound carbonyls and lipid hydroperoxides, which are suggestive of protein and lipid oxidative damage, respectively, can provide dynamic insights into oxidative stress onset mechanisms. The present study integrates both *in vitro* and *in vivo* methods to evaluate the bioavailability of metals and their role in ROS generation and redox homeostasis alterations. In contrast to prior research, this study:

- Standardizes SBF compositions and assay conditions to enhance reproducibility.
- Examines multiple exposure routes, including inhalation, ingestion, and ocular contact.
- Uses *Artemia franciscana* as a model organism to bridge the gap between bioavailability assessments and whole-organism toxicity.

By addressing these gaps, this study aims to provide a comprehensive evaluation of PM-induced toxicity and contribute to the development of more effective air quality regulations. *Artemia franciscana* nauplii were employed due to their widespread availability, ease of cultivation, and physiological sensitivity to pollutants (Azra et al., 2022). Moreover, *Artemia franciscana* offers a cost-effective, ethical alternative to vertebrate models (Chen et al., 2022). Even if *Artemia* is generally used as a model for the study of environmental effects, there are published papers (Chainy et al., 2016; Hamidi et al., 2014; Ntungwe et al., 2020; Rajabi et al., 2015) that suggest the use of this model as an alternative biological assay to conduct toxicological studies on humans. Furthermore, *Artemia franciscana* exhibits sophisticated oxidative stress adaptation mechanisms that parallel those found in higher organisms. The species possesses robust antioxidant systems including both enzymatic components such as glutathione peroxidase and reductase, and non-enzymatic antioxidants, enabling effective management of reactive oxygen species under various environmental challenges (Tomajoli et al., 2025). The use of biologically relevant particle sizes and environmentally realistic PM concentrations enhances the applicability of the findings.

The remainder of the work is organized as follows: In Section 2, we briefly outline the characteristics of the sampling site, and the methods used to obtain PM samples. Particular attention is given to the preparation of extracting solutions using simulated biological fluid and extraction conditions. The results are presented in Section 3, followed by the discussion in Section 4. Finally, the main conclusions are summarized in Section 5.

2. Materials and methods

2.1. Site description and sampling procedure

For this study, samples were collected between June, 2013 and March, 2017. The sampling equipment was positioned on the rooftop of the historical university complex at the San Marcellino Observatory (40.848° N, 14.258° E; 53 m above sea level, Fig. 1). This location, situated in the UNESCO World Heritage-listed downtown area, is affected by diverse pollution sources, including vehicular emissions, port activities, and biomass burning from numerous nearby establishments. Previous studies have characterized PM composition in the Naples urban area (Chianese et al., 2019), providing important baseline data for this location. Although situated within a restricted-traffic zone, the site is less than 200 m from major roads and in close proximity to the marina, both of which contribute to ambient air pollution. Further details about the sampling site can be found in Agrillo et al. (2013), Riccio et al. (2014); (2016); (2017); Riccio et al. (2017) and Dinoi et al. (2017a).

Particulates were collected on quartz microfiber filters (Whatman Q-grade, 47 mm diameter), with each sample representing a 24-hour sampling period. Mass concentrations were determined using the β-ray attenuation method with low-volume samplers (2.3 m^3/h) equipped with dual channels for automatic sampling and monitoring of PM_{10} and $PM_{2.5}$ (SWAM 5a Dual Channel Monitor-FAI Instruments). This method measures the attenuation of β-rays passing through the filter medium, where the attenuation intensity is directly proportional to the particulate matter collected. Measurements obtained via β-ray attenuation showed excellent agreement with those from the standard reference gravimetric method, with a typical daily mass concentration uncertainty of 0.5–0.6 μg/m^3 (Dinoi et al., 2017b).

Fig. 1. Location of the sampling site in Naples (Italy).

2.2. Selection of samples

To reduce the number of samples to be analyzed (the entire monitoring campaign ranged over about four years), and consequently minimize analysis time and costs, a subset of samples was selected. The selection was based on the analysis of backward trajectories, focusing on samples representative of emission sources from specific regions. Back-trajectories were generated using the HYSPLIT 5.3.2 model, developed by the Air Resources Laboratory (ARL) of the National Oceanic and Atmospheric Administration (NOAA). Detailed information about the model is available on the NOAA ARL website (https://www.ready.noaa.gov/HYSPLIT.php) and in related publications (Stein et al., 2015). The meteorological inputs for trajectory calculations were derived from the Global Data Assimilation System (GDAS) of the National Center for Environmental Prediction (NCEP), using 3-hourly data, combined with monitoring data to provide spatiotemporally resolved PM fields in the Naples region (Chianese et al., 2018).This system integrates observational weather data and performs computational analyses to generate forecasts four times daily. Additional information about GDAS is available on the ARL website (https://www.ready.noaa.gov/gdas1.php).

Trajectories started from the monitoring site (40.847342°N, 14.257839°E) and were integrated backward for a five-day (120-hour) period, using 3D wind data from the GDAS archive. Trajectories were launched every hour, resulting in 24 trajectories per day, starting from an altitude of 500 m (near ground). Along each trajectory, data points were recorded every one hour, capturing the three-dimensional position, temperature, humidity, and mixed-layer height at each interval.

Back-trajectories were visually inspected, and a subset corresponding to stagnant conditions in highly urbanized areas was selected. The most probable transport pathways were identified by deriving a probability density field (Ashbaugh et al. 1985; Poirot and Wishinski, 1986). From the set of all sampling days, 52 daily average samples were selected for both PM_{10} and $PM_{2.5}$, during the period from December 2013 to April 2014, when the highest PM concentrations were collected. These samples mostly correspond to air mass trajectories of northern or eastern origin, forming a homogeneous subset in which differences in PM concentrations are more likely influenced by local emissions and meteorological conditions rather than the area of origin.

2.3. Elements of interest

Studies on bioavailability have extensively explored transition metals and metalloids due to their environmental prevalence and biological impacts (Kastury et al., 2017). In this work, we selected Cu, Cd, Pb, Ni, V, As, Zn, and Fe based on their ambient abundance, biological relevance, and regulatory significance (Council of the European Union, 2024).

Fe, Zn, Ni, and Cu were included because of their high concentrations in atmospheric particulate matter (Chen and Lippmann, 2009, Popoola et al., 2018) and their well-documented roles in generating reactive oxygen species (Angelé-Martínez et al., 2014).

Pb and Cd, although present in lower concentrations, were considered due to their interaction with immune cells, particularly phagocytes (Ren et al., 2020). Cadmium is strongly associated with respiratory diseases and exhibits prolonged retention in the human body, exacerbating its toxicological impact (Charkiewicz et al., 2023; Huang et al., 2016). Arsenic was included despite its low concentration in particulate matter, given its high solubility and cytotoxicity, particularly in the context of lung carcinomas (Roig et al., 2013). Similarly, vanadium was examined due to its association with shipping emissions, a significant pollution source in the studied area (Chianese et al., 2022), and its documented cardiovascular toxicity at low concentrations (Jung et al., 2017).

The selection also aligns with the stringent air quality standards established by the recent European directive on air quality (Council of the European Union, 2024). This directive highlights heavy metals such as Pb, As, Cd, and Ni, acknowledging their carcinogenicity and chronic health risks. By converting target values for these pollutants into legally binding limits, the directive underscores the critical need to address these elements in air quality research.

2.4. Analytical procedures for metals extraction and determination

2.4.1. Extraction of metals' total amount

To facilitate multiple analyses, the filters were divided into four equal sections, with each section allocated to a specific extraction procedure. For the determination of the total metal content, one-quarter of the filter was digested in a microwave oven (Milestone Start E) using a mixture of nitric acid and hydrogen peroxide in a 4:2 ratio, as prescribed by the European Standard (CEN-UNI EN 14902:2005, 2005) and detailed in the works of Canepari et al. (2006).

HNO_3 (65 %, Suprapur, Romil) and H_2O_2 (30 %, Suprapur, Carlo Erba) were used for the extraction. Digestion was performed in two stages: in the first stage, the temperature was linearly increased to 220°C for 20 min, followed by a second stage in which the temperature was maintained at 220°C for 25 min.

The resulting solutions were cooled and filtered through nitrate cellulose filters with a pore size of 0.2 μm, then diluted with ultrapure water to a final volume of 10 mL. The solutions were stored at 4°C until analysis.

To account for potential contamination from the filters and reagents, a blank filter section was processed and analyzed using the same procedure. These results were used to correct the metal concentration measurements in the sampled filters.

2.4.2. Extraction of metals using simulated biological fluids

To evaluate the bioavailable fraction of metals, one-quarter of each filter, including blank filters, was treated with specific simulated biological fluids. These fluids included two types of simulated pulmonary fluids (Artificial Lysosomal Fluid [ALF] or Gamble's solution, for $PM_{2.5}$ and PM_{10} respectively), simulated saliva, and simulated tears. Each simulated fluid was prepared using analytical-grade reagents to prevent contamination from trace metals. ALF and Gamble's solutions were prepared following the protocols of Colombo et al. (2008) and Stopford et al. (2003), while saliva and tear solutions were prepared in accordance with Marques et al. (2011) and Duffò and Castillo (2004).

The simulated fluids varied in their chemical composition, organic content, and pH, reflecting different biological environments. ALF is designed to replicate intracellular conditions, particularly within alveolar macrophages, and is characterized by an acidic pH (4.5) and higher organic content. Gamble's solution simulates interstitial lung fluid and contains primarily inorganic salts such as carbonates, chlorides, and phosphates, with a neutral pH (7.4). These differences inform their use in extracting bioavailable metals: ALF was applied to $PM_{2.5}$ due to its ability to penetrate deep into the respiratory tract, while Gamble's solution was used for PM_{10} (Innes et al., 2021). Saliva and tear solutions were applied to both PM fractions to simulate oral and ocular exposure pathways. Their compositions are indicated in Table 1.

To simulate physiological conditions, all extractions were made at 37 °C for 24 h. This timeframe was chosen based on studies indicating that maximum bioavailability is reached within 24 h of particle-fluid interaction (Caboche et al., 2011; Huang et al., 2016). The extraction solutions were manually and intermittently stirred to approximate the conditions of fluid-particle contact in the human body (Wiseman, 2015).

After extraction, all samples were treated with 200 μL of nitric acid and 100 μL of hydrogen peroxide per 10 mL. This pre-treatment step digested organic matter and prevented interference during metal quantification. Metal concentrations in the extracts were then determined using inductively coupled plasma mass spectrometry (ICP-MS), as detailed in Section 2.3.4.

To account for background contamination, blank filters underwent the same extraction process. Results from these blanks were used to correct the measured concentrations in the sample filters, ensuring the accuracy of the reported bioavailable metal fractions.

2.4.3. Extraction conditions

The conditions for extraction—such as temperature, stirring, contact time, and the amount of extraction solution—vary considerably among studies on metal bioavailability.

Typically, extractions are conducted at room temperature or with heated solutions, as discussed by Wiseman (2015). Room-temperature extractions may underestimate metal bioavailability, while heated extractions could overestimate it, since body temperature lies between these extremes. To better simulate physiological conditions, we chose to perform extractions at 37 °C, the human body temperature, aligning with recent studies (Leclercq et al., 2017; Mukhtar and Limbeck, 2013; Wiseman and Zereini, 2014).

Approaches to stirring during extraction also differ. Some studies omit agitation altogether (Huang et al., 2016), while others employ vigorous, continuous shaking to maximize extraction efficiency (da Silva et al., 2015; Leclercq et al., 2017; Li et al., 2017). In this study, we opted for a middle ground: manual shaking at intervals during the contact period. This approach reflects the less-than-optimal mixing conditions in

Table 1
Simulated biological fluids composition.

	ALF (g/L)	Gamble (g/L)	Saliva (g/L)	Tears (mg/100 mL)
Potassium chloride		0.298	0.720	111
Calcium chloride dihydrate	0.128	0.368	0.220	2.29
Sodium chloride	3.21	6.019	0.600	672.8
Potassium phosphate monobasic	-	-	0.680	-
Sodium phosphate dibasic	-	-	0.866	-
Potassium bicarbonate	-	-	1.500	-
Potassium tiocyanate	-	-	0.060	-
Citric acid	20.8	-	0.030	-
Sodium bicarbonate	-	-	-	192.4
Albumin	-	-	-	669
Glucose	-	-	-	2.5
Magnesium chloride	0.050	0.095	-	-
Disodium hydrogen phosphate	0.071	0.126	-	-
Sodium sulphate	0.039	0.063	-	-
Sodium citrate dihydrate	0.077	0.097	-	-
Sodium hydroxide	6.00	-	-	-
Sodium hydrogen carbonate	-	2.604	-	-
Glycine	0.059	-	-	-
Sodium tartrate dihydrate	0.090	-	-	-
Sodium lactate	0.085	-	-	-
Sodium pyruvate	0.086	-	-	-
Sodium acetate	-	0.574	-	-
pH	4.5	7.4	6.5	7.4

the human body, where particle dissolution relies primarily on natural contact with body fluids.

Regarding contact time, studies on dissolution kinetics indicate that over 80 % of $PM_{2.5}$ components dissolve within 8 h in Gamble and ALF solutions (Huang et al., 2016). Maximum bioavailibiliy is typically reached within 24 h in Gamble solution for PM_{10} and $PM_{2.5}$ samples (Caboche et al., 2011). Based on these findings and the limited time particles spend in the human body, we conducted extractions for 24 h. While shorter durations might better mimic contact times for oral and ophthalmic routes, this approach ensures the inclusion of all bioavailable fractions.

The volume of leaching solution was selected with care. According to Caboche et al. (2011) and Boisa et al. (2014), an optimal ratio between sample mass and solution volume (1/500–1/50,000 g/mL, grams of samples for mL of solution) avoids saturation or dilution effects. For this study, we used a ratio of 1/20 g/mL, as ratios above 1/30 g/mL have been shown to reduce the dissolution rate (Caboche et al., 2011). When the solution volumes were less than 10 mL, ultrapure water was added to achieve a final volume of 10 mL. This experimental design aimed to balance practical laboratory constraints with the physiological conditions of metal dissolution in the human body.

2.4.4. Metals determination

Metals determination in all the extracted solutions (about 200 samples) was performed using the EPA 6020 method. Metals concentration was determined using an ICP-MS ELAN 6000 Perkin Elmer instrument, equipped with a cross-flow nebulizer and a Gilson peristaltic pump for sample inlet. The operating conditions were defined as follows: ICP RF Power 1150 W, nebulizer gas flow 0.8 L/min; data acquisition took place by peak hopping with a dwell time of 50 ms.

Instrument optimization was performed daily using a certified PE Pure Perkin Elmer solution with Rh, Mg, Pb (10 μg/L) in a solution of HNO_3 1 %; the calibration of the investigated masses was carried out using 5 standard solutions, at different analyte concentrations, prepared by diluting certified single-element standard solutions PE Pure Plus (Perkin Elmer, Inc, Shelton, USA) in 1 % HNO_3 in the range of 1–200 μg/L. The squared correlation coefficient (R^2) was 0.9999 for each element.

Data on metal concentrations were expressed as the means ± SEM. SEM indicates the Standard Error of the Mean, based on the 95 % confidence interval using a two-tailed *t*-distribution. Moreover, we tested the null hypothesis that data from first and second clusters (originating from northeast and north) have equal medians, using the two-sided Wilcoxon rank sum test, with a significance level of 0.05. Statistical approaches for spatio-temporal air quality data analysis have been advanced through hierarchical Bayesian methodologies (Riccio et al., 2006), which provide robust frameworks for handling the complex spatial and temporal dependencies inherent in atmospheric monitoring data.

2.4.5. Animals

Artemia franciscana (Crustacea, Anostraca) cysts were provided by a commercial shopper (Hobby®, Gelsdorf, Germany). 0.5 g of cysts were incubated for 48 h at 22 °C under constant aeration, with a 16-hour light photoperiod, in 500 mL of artificial seawater (Instant Ocean, 36 ‰) (C). The seawater was supplemented with either 10 mL of extractant buffer for $PM_{2.5}$ and PM_{10} (ALF and Gamble buffers, respectively, referred to as the C(ALF) and C(Gamble) groups) or 10 mL of extract solution derived from PM_{10} (Filters 122, 123, 197) and $PM_{2.5}$ (Filters 296, 298, 300). These latter groups are also identified as Gamble extract and ALF extract groups, respectively. Hatching occurred within a few hours of incubation, and nauplii (instar I-II) were collected after 48 h. Mortality in the control group never exceeded 10 % at 48 h (Motta et al., 2019; Vanhaecke et al., 1981) and was not affected by the treatments.

The nauplii were homogenized using a glass Potter-Elvehjem homogenizer, operated at a standard velocity (500 rpm) for 1 min in ice-cold homogenization medium (0°C) containing 220 mM mannitol, 70 mM sucrose, 1 mM EDTA, and 10 mM Tris (pH 7.4). The protein concentration in the homogenates was measured by the colorimetric Bio-Rad Bradford protein assay, using a commercial kit (Bio-Rad, Hercules, CA, USA), and aliquots were stored to −80°C and used for analytical procedures.

All determinations were performed using three different batches of cysts for each treatment group, with each value representing the mean of two independent measurements.

2.4.6. Redox state evaluations

2.4.6.1. Reactive oxygen species (ROS) content, Oxidative damage to lipids (Hps) and proteins (CO), and in vitro susceptibility to oxidants (ΔHps). The total ROS content was evaluated by a spectrofluorimetric method based on the ROS-induced conversion of 2',7'-dichlorodihydrofluorescein diacetate (DCFH-DA, a non-fluorescent compound) into dichlorofluorescein (DCF, a fluorescent compound), according to Driver et al. (2000). DCFH-DA is commonly used in fluorometric assays to detect a broad spectrum of reactive oxygen species (ROS), including hydrogen peroxide (H_2O_2), lipid hydroperoxides, and peroxynitrite (Driver et al., 2000). However, because it reacts with multiple ROS types, it does not allow for the specific detection of individual ROS molecules. ROS generation can be assessed both in the absence and presence of Fe^{2+}, which amplify ROS generation also inducing the production of short half-life ROS, i.e. through Fenton reaction. The measures were performed on crude homogenate aliquots containing 12.5 μg of proteins and diluted in a 0.1 M monobasic phosphate buffer, pH 7.4, which was firstly incubated with 10 μM DCFH-DA for 15 min, and subsequently with 100 μM $FeCl_3$ for additional 30 min. The conversion of DCFH-DA to fluorescent DCF was measured by using excitation and emission wavelengths of 485 nm and 530 nm, respectively. Background fluorescence (i.e., conversion of DCFH to DCF in the absence of homogenate) was corrected using parallel blanks. ROS content was expressed as Relative Fluorescence Units (RFU) • μg^{-1} proteins.

The extent of lipid peroxidation in nauplii homogenates was assessed by measuring lipid hydroperoxide (Hps) levels in 10 μg of homogenate protein, diluted in 0.1 M monobasic phosphate buffer (pH 7.4) (Heath and Tappel, 1976). Hps content was determined by monitoring the decrease in NADPH absorbance at 340 nm driven by two enzyme-catalyzed reactions. Glutathione peroxidase (GPx, 0.025 U/mL) neutralizes Hps by oxidizing the ~~*antioxidant thiol*~~ reduced glutathione (GSH, 0.425 mM) to oxidised glutathione (GSSG), while glutathione reductase (GR, 0.025 U/mL) regenerates GSH from GSSG by consuming NADPH. Lipid hydroperoxide levels were expressed as nmol NADPH oxidized·min^{-1} ·mg^{-1} protein.

Protein oxidative damage was evaluated by quantifying protein-bound carbonyls (CO) through their reaction with 10 mM 2,4-dinitrophenylhydrazine (DNPH), using a simplified method adapted for a Nunc standard 96-well plate (Mesquita et al., 2014). Briefly, 40 μL of homogenate, previously treated with a lysis buffer (100 mM NaH_2PO_4 (phosphate buffer) containing 0.2 % digitonin, 80 μg/mL Phenylmethanesulfonyl fluorid (PMSF), 10 μg/mL leupeptin, 14 μg/mL pepstatin, 10 μg/mL aprotinin, pH 7.4) and 1 % streptomycin, was centrifuged at 600 g at 4°C for 10 min, and incubated with an equal volume of 40 mM DNPH (dissolved in 2.5 N HCl) at room temperature for 10 min. Next, 20 μL of sodium hydroxide (6 N) was added, and the mixture was incubated for an additional 10 min at room temperature. Subsequently, 185 μL of phosphate buffer was added to 25 μL of the sample and absorbance was read at 450 nm. Protein carbonyls content was calculated using the DNPH extinction coefficient at 450 nm (ε = 22, 308 M^{-1} cm^{-1}) with an optical path length of 0.1 cm and expressed as μmol CO·mg^{-1} protein. Total homogenate protein was determined using the Bradford reagent following the manufacturer's instructions (Bio--Rad, USA).

The *in vitro* susceptibility to oxidizing agents was evaluated by the

change in Hps (ΔHps) levels induced by treating 0.01 mg of proteins from *Artemia franciscana* homogenates with a mixture of iron and ascorbate (Fe/As) at a concentration of 100/1000 μM for 10 min at room temperature. Ascorbate reduces iron, and the Fe^{2+} reacts with the Hps of the samples producing hydroxyl radical that, if not scavenged by the sample's antioxidants, triggers lipid peroxidation. The reaction was stopped by adding 0.2 % 2, 6-di-t-butyl-p-cresol (BHT). All the biomarkers were evaluated by using a microplate reader (Synergy™ HTX Multimode Microplate Reader, BioTek Santa Clara, CA, USA).

2.4.6.2. Activity of the antioxidant enzymes Glutathione Peroxidase (GPx) and Glutathione Reductase (GR). GPx activity was spectrophotometrically measured by following the rate of NADPH (1.5 mM) oxidation of 0.02 mg of proteins obtained in the presence of H_2O_2 (1.5 mM) as substrate, GSH (10 mM) and GR (2.4 U/mL) in 0.1 M KH_2PO_4, 1 mM EDTA, pH 7.0 (Flohé and Günzler, 1984). GPx activity was expressed as μmol NADPH oxidized • min^{-1} • mg-^{1} proteins.

GR activity was spectrophotometrically assayed by measuring the rate of NADPH (2 mM) oxidation of 0.02 mg of proteins after the addition of 20 mM GSSG in 0.2 M KH_2PO_4, 2 mM EDTA, pH 7.0 (Carlberg and Mannervik, 1985). GR activity was expressed as μmol NADPH oxidized • min^{-1} • mg^{-1} proteins.

All the biomarkers were evaluatedby using a microplate reader (Synergy™ HTX Multimode Microplate Reader, BioTek Santa Clara, CA, USA).

2.4.6.3. Data Analysis. Data related to the redox state evaluation were expressed as the means ± SEM of three batches of nauplii hatched under each experimental condition. Each value represents the media of two technical replicates. Equal Variance was assessed by Brown-Forsythe test. Data were analyzed by one-way ANOVA followed by Tukey's pairwise comparison tests (Graph Pad Prism 8, GraphPad Software, La Jolla California, USA). The *p*-values of $*p < 0.5$, $**p < 0.01$, $***p < 0.001$, and $****p < 0.0001$ were assigned to indicate statistical significance between the different experimental groups.

3. Results

3.1. Particulate matter daily concentration

In Table 2, a detailed statistical analysis of $PM_{2.5}$, PM_{10} and PM_{coarse} (the difference between PM_{10} and $PM_{2.5}$) concentrations, including their ratios, is shown. The statistical metrics—mean, standard deviation, and ranges (minimum and maximum values)—emphasize the variability and concentration levels of particulate matter over the study period.

Mean concentrations of 17.3 ± 7.5 μg/m^3 ($PM_{2.5}$) and 23.8 ± 9.0 μg/m^3 (PM_{10}) show that fine particles form a significant portion of total PM. The PM_{10}/ $PM_{2.5}$ ratio, averaging 0.7, corroborates the dominance of fine particles in the urban aerosol composition, consistent with findings in similar Mediterranean urban regions (Kanakidou et al., 2011; Rodríguez et al., 2007). The health implications of these concentrations are considerable, as $PM_{2.5}$ particles are known to penetrate deep into the respiratory tract, bypassing defense mechanisms, reaching alveolar regions and carrying toxic metals and organic compounds (Huang et al., 2016; Andreyev et al., 2005). This ratio also suggests significant anthropogenic contributions, such as vehicular emissions and industrial processes, as major sources of fine particulate matter.

Table 2
Statistical values for $PM_{2.5}$ and PM_{10} (μg/m^3).

	$PM_{2.5}$	PM_{10}	PM_{coarse}	PM_{10}/ $PM_{2.5}$
mean	17.3	23.8	6.6	0.7
std	7.5	9.0	3.9	0.1
min	6.6	11.6	3.2	0.5
max	33.6	41.1	20.7	0.8

The elevated maximum values—33.6 μg/m^3 for $PM_{2.5}$ and 41.1 μg/m^3 for PM_{10}—highlight episodic pollution events, potentially linked to specific meteorological conditions or short-term emission surges. When compared to recent European air quality standards (European Union, (2024)), $PM_{2.5}$ exceeded the threshold (25 μg/m^3) only four times during the monitoring period, while PM_{10} did not exceed its limit (45 μg/m^3). However, although PM_{10} does not exceed legal limits and is less bioavailable than $PM_{2.5}$, it may pose substantial risks by acting as a carrier for hazardous constituents.

Following the methods of Ashbaugh et al. (1985) and Poirot and Wishinski (1986), the subset of samples corresponding to eastern and northern trajectories was used to reconstruct the corresponding probability density function (*pdf*) of residence times. This *pdf* represents the likelihood of air parcels spending time in specific regions, helping to identify pollution sources on the days when samples were collected, as illustrated in Fig. 1. Areas marked in red highlight regions from which air masses are more likely to originate. The contour intervals are plotted on a logarithmic scale using a grid at a spatial resolution of 25 × 25 km^2. During the sampling period, the region most frequently traversed by air parcels *en route* to the receptor site is marked by the ridge in the contour pattern that spans the meridional and central areas of Italy. These regions encompass highly populated and industrialized areas, suggesting that the samples collected at the receptor point reflect a diverse range of sources, predominantly of anthropogenic origin. The highest probability of air parcel trajectories originates from the north and northeast, primarily covering Italy and Eastern European regions. In contrast, lower probabilities are associated with trajectories from the south and southwest, including northern Africa and the Iberian Peninsula.

3.2. PM_{10} and $PM_{2.5}$ elemental composition

Fig. 3 shows the elements' distribution between fine and corse fraction, highlighting the differences in metal concentrations between the two particle size fractions. The results indicate that fine particles consistently exhibit higher concentrations of transition metals such as Cu, Zn, and Fe compared to coarser particles (PM_{coarse}). This observation aligns with existing literature, which emphasizes the toxicological significance of fine particulate-bound metals due to their ability to generate reactive oxygen species (ROS) through Fenton-like reactions, leading to oxidative stress and cellular damage (Valavanidis et al., 2005).

The most abundant element is Fe (averaging 649 ± 88.0 ng/m^3 in PM_{10} and 452 ± 48.0 ng/m^3 in $PM_{2.5}$), followed by Pb (26.3 ± 3.90 ng/m^3 in PM_{10} and 22.9 ± 3.10 ng/m^3 in $PM_{2.5}$), Cu (20.4 ± 6.20 ng/m^3 in PM_{10} and 13.4 ± 5.30 ng/m^3 in $PM_{2.5}$) and Zn (14.0 ± 1.50 ng/m^3 in PM_{10} and 13.6 ± 1.60 ng/m^3 in $PM_{2.5}$). Other elements are present in lower concentrations; in the order: As (4.80 ± 0.90 ng/m^3 in PM_{10} and 4.30 ± 0.70 ng/m^3 in $PM_{2.5}$) > Cd (2.50 ± 0.30 ng/m^3 in PM_{10} and 2.30 ± 0.30 ng/m^3 in PM_{10}) > V (2.30 ± 1.10 ng/m^3 in PM_{10} and 2.10 ± 0.90 ng/m^3 in $PM_{2.5}$) > Ni (2.00 ± 0.60 ng/m^3 in PM_{10} and 1.70 ± 0.50 ng/m^3 in $PM_{2.5}$).

It is noteworthy that the elevated presence of redox-active metals like Cu and Fe in both PM_{10} and $PM_{2.5}$ fractions is particularly significant, given their role in promoting ROS generation. The high concentrations of these metals in $PM_{2.5}$ suggest that fine particles, due to their smaller size and greater surface area, are more efficient carriers of toxic metals, allowing deeper penetration into the respiratory system and increasing potential health risks. Similarly, Pb, while present in both fractions, is predominantly found in the fine fraction, further emphasizing its toxic potential.

The levels of both Ni and V can be attributed to the combustion of heavy fuel oils, consistent with their known emission profiles in urban and peri-urban environments. The V/Ni ratio in the range of 2.5–3.5–4.0 is considered a typical combustion marker for ship engines (Viana et al., 2009), whereas ratios below 2 are commonly associated with Ni-rich atmospheric pollution sources (Moreno et al., 2010). In this study, the V/Ni ratio falls within the range of 0.9–1.6.

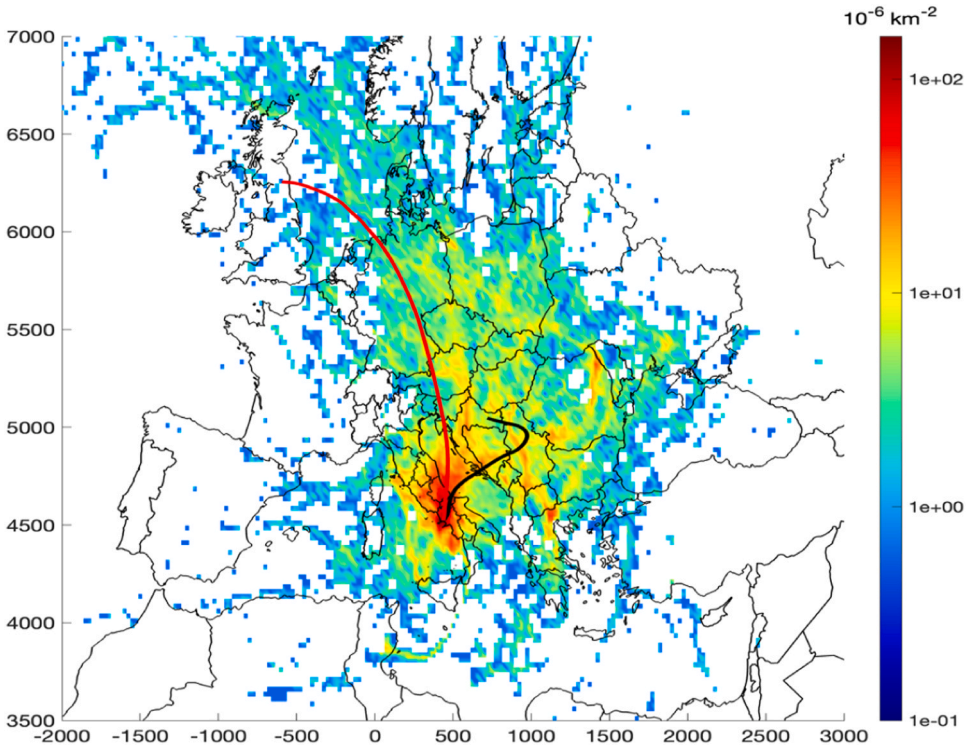

Fig. 2. The residence time analysis. This map uses colors to indicate the probability of origin. Superimposed are two lines, marked in red and black, representing the average directions from the northern and north-eastern sectors.

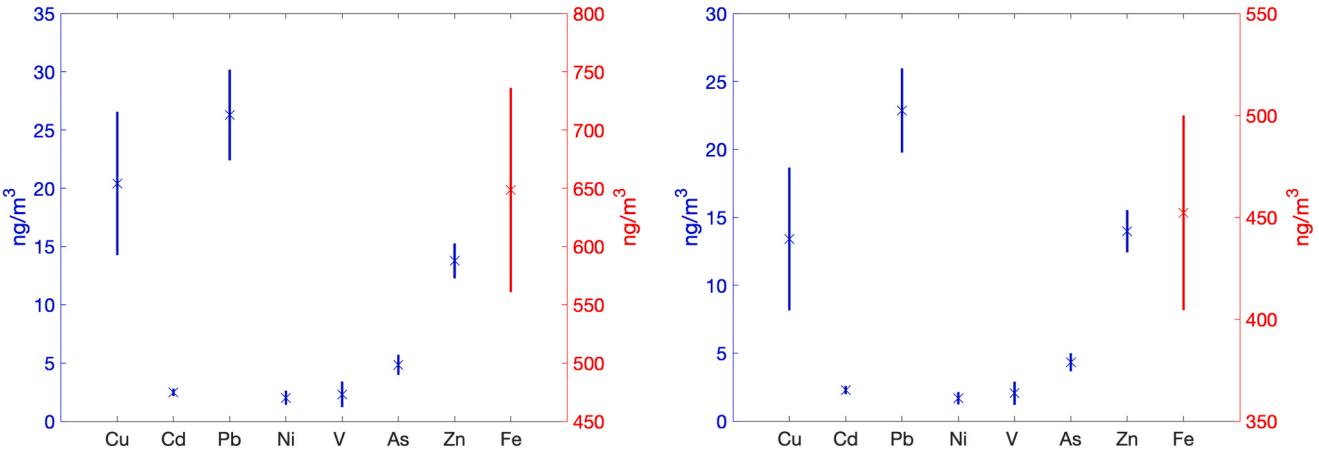

Fig. 3. (a.) Metal distribution in the PM_{10} fractions. The 'x' crosses represent the mean values, and the vertical bars indicate the corresponding standard errors at a significance level of 0.05. The elements displayed in blue correspond to the scale on the left side; iron (in red) corresponds to the scale on the right. Fig. 3b. Metal distribution in the $PM_{2.5}$ fractions. The 'x' crosses represent the mean values, and the vertical bars indicate the corresponding standard errors at a significance level of 0.05. The elements displayed in blue correspond to the scale on the left side; iron (in red) corresponds to the scale on the right.

The statistical values (mean, minimum and maximum) for $PM_{2.5}$ and PM_{10} in each cluster are reported in Table 3. According to the Wilcoxon test, differences in the median between the northeast and north clusters were not significant at a 0.05 level for all elements, except for lead in the $PM_{2.5}$ fraction and arsenic in the PM_{10} fraction, whose differences were marginally significant.

3.3. *Bioavailability of metals in simulated solutions*

The bioavailability of metals in airborne particulate matter is a critical determinant of their potential toxicity and subsequent health risks. The bioavailability of metals extracted from particulate matter (PM_{10} and $PM_{2.5}$) was evaluated using simulated biological fluids to replicate different human exposure pathways. The fraction of bioavailable metals, expressed as a percentage of the total content, is presented in Fig. 4.

Since PM_{10}, due to its larger particle size, primarily deposits in the tracheobronchial and alveolar regions (Kastury et al., 2017), Gamble's solution was used in this study to assess the bioavailibiliy of PM_{10} only. Conversely, finer particles such as $PM_{2.5}$ are more prone to phagocytosis by alveolar macrophages; therefore, ALF was selected to evaluate $PM_{2.5}$ bioavailibiliy (Wiseman, 2015). Simulated tears and saliva were used to assess the bioavailibiliy of both size fractions.

The results indicate that metal solubility varied significantly across different fluids, with pH and fluid composition playing key roles in modulating bioavailability. ALF, characterized by its acidic pH (4.5),

Table 3
Statistical values for $PM_{2.5}$ and PM_{10} (ng/m^3).

				NORTHEAST				
	Cu	**Cd**	**Pb**	**Ni**	**V**	**As**	**Zn**	**Fe**
$PM_{2.5}$	ng/m^3	ng/m^3	ng/m^3	ng/m^3	ng/m^3	ng/m^3	ng/m^3	ng/m^3
median	17,4	2,1	20,3	1,60	1,40	3,70	13,0	459
minimum	4,00	1,00	9,30	0,70	0,60	0,70	4,90	272
maximum	59,6	3,60	37,5	2,40	2,70	6,00	21,1	702
	Cu	Cd	Pb	Ni	V	As	Zn	Fe
PM_{10}	ng/m^3	ng/m^3	ng/m^3	ng/m^3	ng/m^3	ng/m^3	ng/m^3	ng/m^3
median	23,7	2,30	23,9	1,60	1,40	3,80	12,5	560
minimum	6,30	0,70	15,5	1,20	0,80	1,20	4,50	377
maximum	67,0	4,20	55,6	2,90	3,40	7,80	21,5	806
					NORTH			
	Cu	**Cd**	**Pb**	**Ni**	**V**	**As**	**Zn**	**Fe**
$PM_{2.5}$	ng/m^3	ng/m^3	ng/m^3	ng/m^3	ng/m^3	ng/m^3	ng/m^3	ng/m^3
median	8,70	2,50	25,9	1,80	2,80	5,10	15,2	444
minimum	4,90	1,60	15,5	0,40	0,60	2,60	11,6	292
maximum	13,4	3,00	31,8	6,20	10,5	6,70	18,4	688
	Cu	**Cd**	**Pb**	**Ni**	**V**	**As**	**Zn**	**Fe**
PM_{10}	ng/m^3	ng/m^3	ng/m^3	ng/m^3	ng/m^3	ng/m^3	ng/m^3	ng/m^3
median	17,6	2,70	28,3	2,4	3,10	5,70	14,9	723
minimum	9,40	2,20	20,8	0,77	0,80	1,60	12,8	348
maximum	30,0	3,50	34,1	6,90	11,1	8,70	16,8	1183

exhibited the highest capacity for metal dissolution, particularly for transition metals such as iron (Fe), copper (Cu), and nickel (Ni). The chemical composition of ALF solution mimics the phagolysosomal conditions within alveolar macrophages, where inhaled particles are internalized and exposed to proton-rich environments. This facilitates the dissolution of metal species through acid-promoted leaching mechanisms, which are known to enhance the release of redox-active metals that contribute to oxidative stress (Wiseman, 2015; Kastury et al., 2017). The higher solubility observed for Fe in ALF compared to other fluids is particularly relevant, as Fe-mediated Fenton reactions have been implicated in the generation of reactive oxygen species (Li et al., 2002).

Conversely, Gamble's solution, which maintains a neutral pH (7.4) and simulates the interstitial lung fluid of the respiratory tract, exhibited a lower solubilization efficiency for transition metals. Some elements, e.g. Cu and Fe, retain a certain degree of bioavailibiliy in this fluid, suggesting that neutral pH conditions may still favor the dissolution of certain metal species. Lead (Pb) is slightly soluble in Gamble's solution. This result aligns with previous studies showing that Pb solubilization strongly depends on pH and ligand complexation, with acidic conditions enhancing its mobilization from atmospheric PM, although some mobilization under neutral conditions cannot be ruled out (Boisa et al., 2014). The greater solubility of Pb in ALF compared to Gamble's solution suggests that Pb-containing mineral phases in PM are more prone to dissolution in the intracellular environment than in extracellular pulmonary fluids, which has important implications for systemic lead uptake following inhalation.

For simulated oral exposure, saliva was employed as a representative fluid to assess the bioavailability of metals through ingestion pathways. The results demonstrated that saliva exhibited limited extraction efficiency for most metals, except for Zn and Fe. The presence of bicarbonates and phosphates in saliva may also contribute to metal precipitation, further limiting bioavailability. The enhanced solubility of Zn in saliva compared to other elements is noteworthy, as Zn is an essential trace element that exists predominantly in bioavailable forms and is often associated with anthropogenic sources such as vehicular emissions and industrial activities (Chianese et al., 2019). Given the physiological role of Zn in cellular homeostasis, its higher solubility in saliva compared to other toxic metals may be indicative of differential bioavailibiliy mechanisms that prioritize the mobilization of essential over non-essential elements.

In the context of ocular exposure, simulated tears were utilized to evaluate the bioavailibiliy of metals upon contact with the eye's surface. The results revealed significant variability in metal solubility, with V and Zn displaying the highest bioavailability in this medium. The enhanced extraction of V in simulated tears aligns with previous observations that vanadate species exhibit high aqueous solubility and remain mobile under physiological conditions (Jung et al., 2017). Given that vanadium is frequently associated with fuel combustion sources, its solubility in tear fluid raises concerns about potential ocular toxicity upon exposure to PM-enriched environments, particularly in urban and industrialized settings (Chianese et al., 2022). The lower bioavailibiliy of Cd, Pb and Ni in tear fluid compared to other media suggests that the ionic strength and composition of this fluid may not favor the dissolution of these elements, thereby reducing their potential for direct ocular absorption.

Considering that the greatest recovery percentages of metals were reached with simulated pulmonary fluids, we used the extracts obtained with these solutions to conduct experiments with the animals to study the toxicity induced by particles.

3.3.1. *Tests with artemia franciscana*

Fig. 5 shows ROS content (Panel A), lipid hydroperoxides (HPs) (Panel B) and protein-bound carbonyl (CO) (Panel C) levels, and *in vitro* susceptibility to oxidants (ΔHPs) (Panel D). The cysts' incubation with extracting buffers for PM_{10} and $PM_{2.5}$ did not influence any of the parameters relating to the samples' redox state. ROS content, HPs and CO levels significantly increased under exposure to PM_{10} and $PM_{2.5}$ extracts compared to all control groups. Interestingly, $PM_{2.5}$ extract exposure significantly increased HPs and CO levels with respect to the group exposed to PM_{10} extract. *In vitro* susceptibility to oxidants followed the trend of Hps and CO content, showing a greater susceptibility to oxidative damage in nauplii hatched after exposure to particulate matter extracts.

Fig. 6 shows Glutathione peroxidase (GPx) (Panel A) and Glutathione reductase (GR) (Panel B) activities measured in nauplii homogenates. The activities of both antioxidant enzymes resulted unmodified in nauplii of control group and nauplii hatched after exposure to PM_{10} and $PM_{2.5}$ extracts. The treatment of the cysts with ALF and Gamble extracts significantly increased both GPx and GR activities compared to the respective control groups with highest values in the nauplii homogenates hatched under exposure to fine particles.

4. Discussion

The findings of this study emphasize the differential bioavailability and toxicity of PM_{10} and $PM_{2.5}$, highlighting their physicochemical

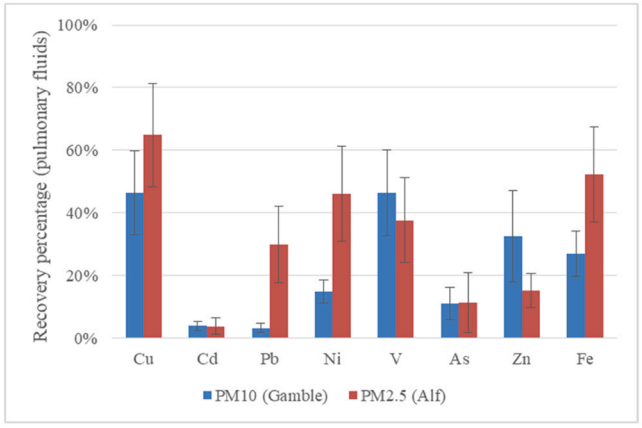

a)

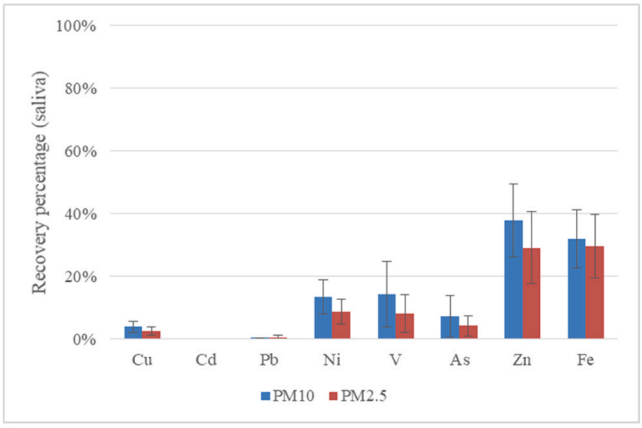

b)

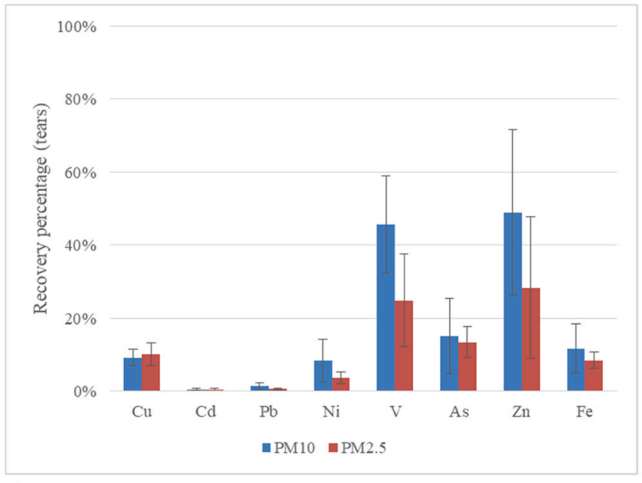

c)

Fig. 4. a-Bioavailability of elements in simulated ALF (PM2.5 fraction) and Gamble (PM10 fraction) solution; b- Bioavailability of elements in simulated saliva solution; c-Bioavailability of elements in simulated tears solution.

properties and associated health risks. The bioavailability of metals in PM plays a critical role in toxicity, as bioavailable fractions significantly contribute to reactive oxygen species (ROS) generation, leading to oxidative stress and subsequent cellular damage (Valavanidis et al., 2005; Kehrer and Klotz, 2015).

The bioavailability of metals was assessed using simulated biological fluids to mimic different human exposure routes. The results revealed that acidic environments, such as artificial lysosomal fluid (ALF, pH 4.5), significantly enhanced the solubility of Pb, Fe, Cu, and Ni, confirming previous findings that lower pH increases metal bioavailibiliy through proton-promoted leaching mechanisms (Wiseman, 2015; Kastury et al., 2017). Gamble's solution (pH 7.4), which simulates interstitial lung fluid, exhibited lower solubilization efficiency, particularly for redox-active metals, but still facilitated the dissolution of Cu and Fe. The higher solubility of Pb in ALF compared to Gamble's solution suggests an increased risk of systemic Pb uptake following inhalation exposure (Chen and Lippmann, 2009).

The bioavailability of metals in simulated saliva and tears provided insights into oral and ocular exposure pathways. Zn and Fe exhibited higher solubility in saliva, possibly due to their essential biological roles and, consequently, naturally bioavailable forms. In contrast, V, a known toxicant associated with combustion sources, demonstrated the highest bioavailability in simulated tears, raising concerns about ocular toxicity in urban environments (Jung et al., 2017). The low bioavailibiliy of Ni and Pb in tear fluid suggests that these elements are less prone to dissolution under ocular conditions, reducing their potential for absorption via eye exposure.

Toxicological assessments conducted using *Artemia franciscana* nauplii hatched under Gamble and ALF extracts further corroborate the *in vitro* bioavailability findings, reinforcing the link between metal solubility and redox state alterations in the whole organism. These alterations are due to the increased ROS content. The presence of redox-active transition metals (Fe and Cu) in our Gamble and ALF extracts, which participate in the Haber-Weiss reaction with sample hydroperoxides, can account for the elevated ROS levels observed. These ROS include highly reactive species such as hydroxyl and superoxide radicals, which react almost immediately upon formation, as well as less reactive species like hydrogen peroxide, which can still induce oxidative damage if released into the cytosol (Napolitano et al., 2021). Cadmium does not directly generate free radicals, but studies showed that it can induce nitric oxide, superoxide, and hydroxyl radical production primarily by displacing Fe and Cu from cytoplasmic and membrane proteins, making them prone to participate in Fenton chemistry (Waisberg et al., 2003; Wätjen and Beyersmann, 2004). Also, arsenic exposure may also lead to radical, reactive nitrogen species, and peroxyl radical formation (Shi et al., 2004). Finally, we can't exclude that metal-redox interactions between Fe, Ni, Cu, and organic components such as polycyclic aromatic hydrocarbons (PAHs) contribute to the generation of secondary radicals, amplifying the toxicological effects of PM exposure (Squadrito et al., 2001; Li et al., 1995)

Our findings show that the increased ROS content induces oxidative damage to lipids and proteins in *Artemia franciscana* nauplii homogenates, highlighting the potential health risks posed by metal-enriched PM exposure (Pham-Huy et al., 2008). ROS react with lipids to trigger a series of chain reactions, lipid peroxidation. (Napolitano et al., 2019). This process prompts cell membrane damage and generates reactive by-products that can further damage the cell (Mylonas and Kouretas, 1999). The higher lipid peroxidation induced by ALF compared to Gamble extracts agrees with the observation that fine particulates release more redox-active elements. Moreover, *in vivo*, the small size of $PM_{2.5}$ and the greater surface area amplify toxicity, facilitating interactions with cellular membranes and enhancing oxidative damage (Dahl et al., 2015). The highest HPs content in nauplii homogenates hatched after ALF extracts exposure also aligns with the highest *in vitro* susceptibility to oxidants. It is reported that $PM_{2.5}$ and PM_{10} can also affect protein activity directly or indirectly, since they are responsible for nitrosylation, carbonylation, disulfide bond formation, and glutathionylation of proteins (Sharma et al., 2012). Alternatively, proteins can conjugate with breakdown products of fatty acid peroxidation (Sharma et al., 2012). Thus, site-specific amino acid modification, fragmentation of the peptide chain, aggregation of cross-linked reaction products, alter electric charge, and increase susceptibility of proteins to proteolysis (Sharma et al., 2012). The exposure of cysts to ALF and Gamble extracts also affects the antioxidant system of the nauplii. ROS are not only molecules able to induce oxidative damage to biological

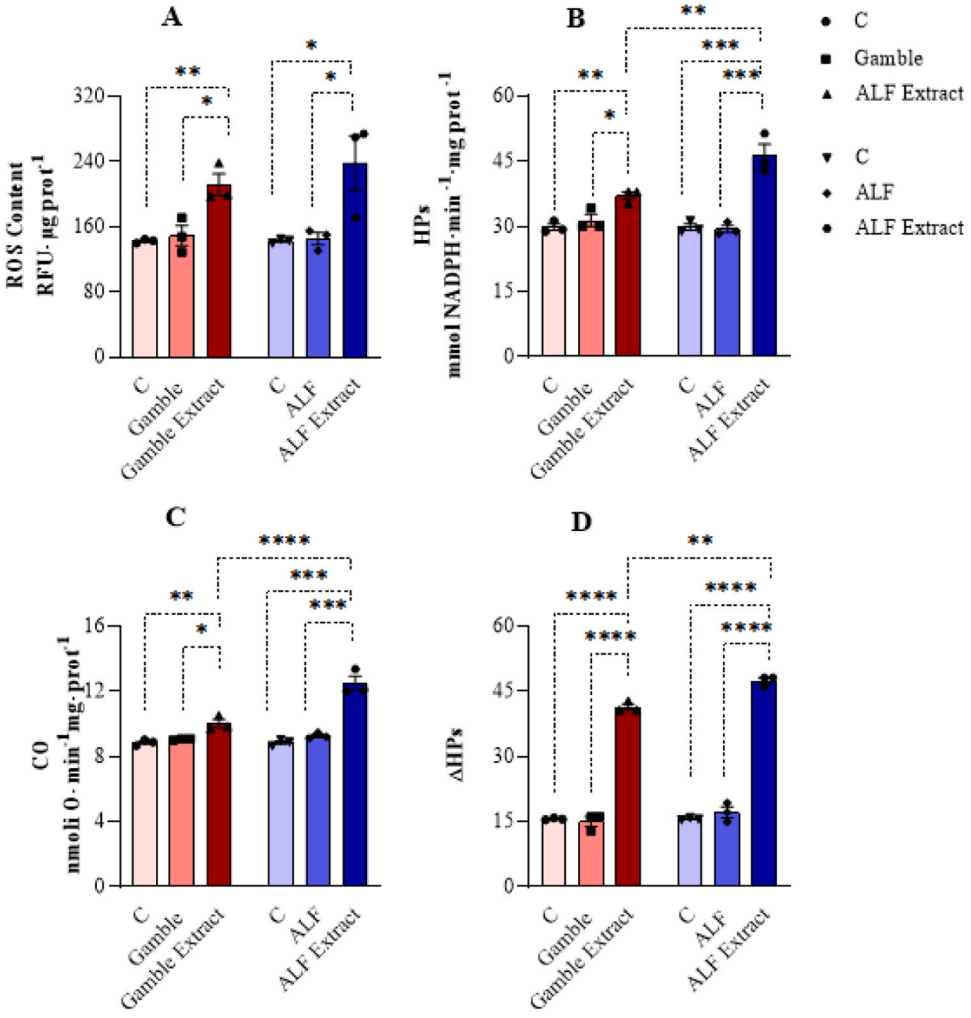

Fig. 5. ROS content, oxidative damage markers to lipids (HPs) and proteins (CO) and *in vitro* susceptibility to oxidants (ΔHPs) of nauplii homogenates of Control group (C) and homogenates of nauplii hatched under Gamble, ALF, Gamble Extracts and ALF extract groups. ROS content was expressed as Relative Fluorescence Units • µg protein^{-1} (Panel A); HPs levels were expressed as nmol NADPH oxidized•min^{-1}• mg^{-1} protein (Panel B); CO levels were expressed as µmol of protein-bound carbonyls• mg^{-1} protein (Panel C);ΔHPs (Panel D). Values are means ± SEM of three different batches of cysts and each value is the media of two technical replicates.

macromolecules but are also signaling molecules able to activate the transcription of genes involved in the redox homeostasis, among which those ones involved in the activation of antioxidant defense system (Napolitano et al., 2021). Therefore, we can speculate that the increased ROS content of nauplii hatched under particulate exposure can induce an adaptative response involving an increased activity of GPx and GR, antioxidant enzymes essential for maintaining GSH/GSSG ratio, being GSH the main soluble cellular antioxidant (Napolitano et al., 2021). It is reported that the activation of the antioxidant system is a physiological response to the increased cellular ROS content (Napolitano et al., 2022). Moreover, we can't exclude a direct action of the metals bioavailable in both the particulate extracts on the antioxidant enzymes. Zinc is widely recognized for its antioxidant properties (Powell, 2000). It can regulate total cellular glutathione concentration by upregulating glutamate-cysteine ligase, a key enzyme in glutathione synthesis (Foster and Samman, 2010). Zinc also enhances glutathione peroxidase activity (Mariani et al., 2008). The highest GPx and GR activities in the group of homogenates obtained from cysts exposed to ALF extracts reflect the higher oxidative damage and susceptibility to oxidants respect to the experimental group exposed to Gamble extract.

In the whole, our toxicological assessment highlighted a deep impact of bioavailable metals' fraction of both particulate matters on the redox homeostasis of the experimental model *Artemia franciscana*, with major alterations induced by fine particulate, that can be explained by the higher metal availability compared with coarse particulate. Given that $PM_{2.5}$ exhibits higher toxicity due to enhanced metal bioavailability, targeted interventions focusing on fine particulate control are critical to reducing health risks in urban areas (Dinoi et al., 2017a). The presence of Ni and V in both PM_{10} and $PM_{2.5}$ too suggests contributions from combustion processes, particularly vehicular and shipping emissions (Moreno et al., 2010; Viana et al., 2009), highlighting new attention on the regulation also for these kinds of emissions.

The European Directive on Ambient Air Quality (Council of the European Union, 2024) has established stringent limits for Pb, As, Cd, and Ni, recognizing their carcinogenicity and chronic toxicity. Our results confirm that regulated metals exceed bioavailability thresholds in both PM fractions, reinforcing the necessity of air pollution mitigation strategies to minimize human exposure.

5. Conclusions

The study underscores the significant toxicological implications of particulate matter (PM), particularly $PM_{2.5}$, due to its higher bioavailability of metals and its capacity to induce oxidative stress, a known precursor to various pathological conditions.

The results confirm that $PM_{2.5}$ is more potent in mobilizing redox-

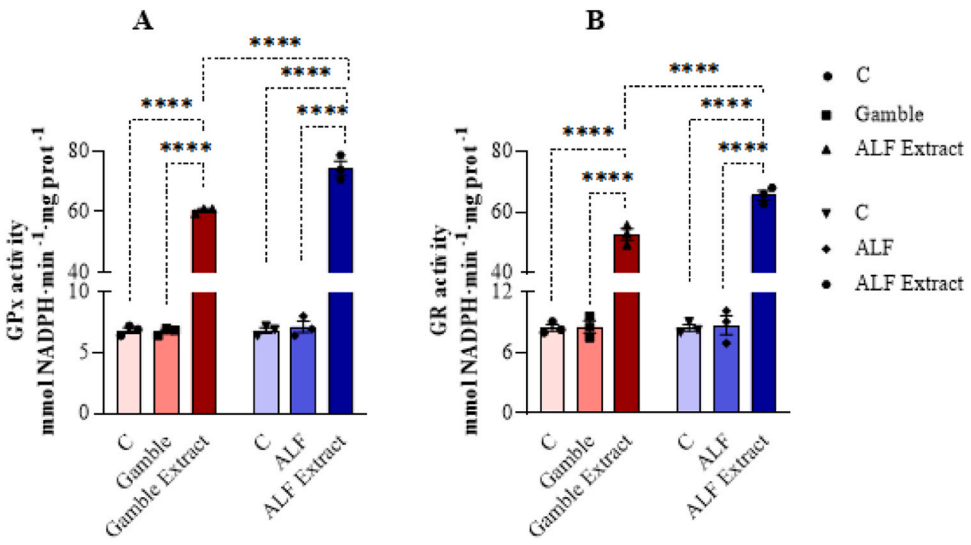

Fig. 6. Antioxidant enzymes' activity of nauplii homogenates of Control group (C) and homogenates of nauplii hatched under Gamble, ALF, Gamble Extracts and ALF extract groups. Glutathione Peroxidase (GPx, Panel A) and Glutathione Reductase (GR, Panel B) activities were expressed as nmol NADPH oxidized•min^{-1}• mg^{-1} protein. Values are means ± SEM of three different batches of cysts and each value is the media of two technical replicates.

active metals such as Fe, Cu, and Zn, which play a pivotal role in reactive oxygen species generation. This process enhances oxidative stress and contributes to cellular damage, aligning with prior research on fine particulate toxicity. In contrast, PM_{10}, while still toxic, exhibits a lower degree of bioavailability for heavy metals, leading to a relatively reduced toxic impact. These findings emphasize the necessity of size-segregated toxicological analyses, which allow for a more precise understanding of PM-associated health risks.

The experimental data obtained using *Artemia franciscana* as an *in vivo* model organism provides compelling evidence of PM-induced toxicity. This study validates the use of *Artemia franciscana* as a cost-effective and ethically viable model, demonstrating its reliability in assessing PM-mediated oxidative damage to lipids and proteins. The significant elevation of lipid hydroperoxides (HPs) and protein-bound carbonyls (CO) following $PM_{2.5}$ exposure indicates an imbalance in redox homeostasis, reinforcing the hypothesis that fine particulate matter is a critical driver of oxidative stress pathways in biological systems.

From an environmental and public health perspective, the differentiation between $PM_{2.5}$ and PM_{10} in terms of bioavailability and toxicity underscores the urgent need for stricter air quality regulations. Current policies largely focus on total metal concentrations, but this study highlights that such an approach may be insufficient in fully assessing environmental risks. Instead, bioavailability assessments should be integrated into regulatory frameworks to better reflect the true toxicological potential of airborne particulates.

In conclusion, although determining the total metal content allows for the identification of exceedances of regulatory thresholds, it is insufficient to assess the environmental risk posed by the mobility and bioavailability (i.e., effective potential toxicity) of heavy metals.

Future research should focus on the long-term health effects of PM exposure, incorporating multi-organism toxicity models to enhance risk assessments. Additionally, the integration of molecular biomarkers and epidemiological data could provide a more comprehensive understanding of PM-induced health impacts. Given the global burden of air pollution-related diseases, these findings contribute to evidence-based policymaking and support targeted mitigation strategies aimed at protecting public health.

CRediT authorship contribution statement

Gianluca Fasciolo: Investigation, Data curation. **Paola Venditti:** Writing – original draft, Data curation. **Angelo Riccio:** Writing – review & editing, Writing – original draft, Methodology, Formal analysis, Data curation, Conceptualization. **Juri Rimauro:** Writing – original draft, Investigation, Data curation. **Gaetana Napolitano:** Writing – original draft, Investigation, Formal analysis, Data curation. **Elena Chianese:** Writing – review & editing, Writing – original draft, Methodology, Investigation, Formal analysis, Data curation, Conceptualization.

Declaration of Competing Interest

The authors declare that they have no known competing financial interests or personal relationships that could have appeared to influence the work reported in this paper.

Acknowledgment

The authors are grateful to the Meteorological Observatory of San Marcellino for hosting instruments and staff during the monitoring campaign. This paper was financially supported by the SCITILLA Project, in the framework of the manifestation of interest for the identification of state universities in Campania for the activation of Research Agreements aimed at improving air quality and reducing PM10 emissions - D.D. n. 283 of 06.06.2024 - Research financed with funds from the Programme Agreement on the Protection of Quality in the Region of Campania/MASE.

Data availability

Data will be made available on request.

References

Agrillo, G., Chianese, E., Riccio, A., Zinzi, A., 2013. Modeling and Characterization of Air Pollution: Perspectives and Recent Developments with a focus on the Campania Region (Southern Italy). Int. J. Environ. Res. 7 (4), 909–916.

Ali, M.U., Liu, G., Yousaf, B., Ullah, H., Abbas, Q., Munir, M.A.M., 2019. A systematic review on global pollution status of particulate matter-associated potential toxic elements and health perspectives in urban environment. Environ. Geochem. Health 41, 1131–1162.

Andreyev, Y., Kushnareva, Y.E., Starkov, A.A., 2005. Mitochondrial metabolism of reactive oxygen species. Biochemistry 70 (2), 200–214.

Angelé-Martínez, C., Goodman, C., Brumaghim, J., 2014. Metal-mediated DNA damage and cell death: mechanisms, detection methods, and cellular consequences. Metallomics 6 (8), 1358–1381.

Ashbaugh, L.L., Malm, W.C., Sadeh, W.Z., 1985. A residence time probability analysis of sulfur concentrations at Grand Canyon National Park. Atmos. Environ. (1967) 19 (8), 1263–1270.
Azra, M.N., Noor, M.I.M., Burlakovs, J., Abdullah, M.F., Abd Latif, Z., Yik Sung, Y., 2022. Trends and new developments in Artemia research. Animals 12 (18), 2321.
Boisa, N., Elom, N., Dean, J.R., Deary, M.E., Bird, G., Entwistle, A., 2014. Development and application of an inhalation bioaccessibility method (IBM) for lead in the PM_{10} size fraction of soil. Environ. Int. 70, 132–142.
Caboche, J., Esperanza, P., Bruno, M., Alleman, L.Y., 2011. Development of an *in vitro* method to estimate lung bioaccessibility of metals from atmospheric particles. J. Environ. Monit. 13 (3), 621–630.
Canepari, S., Cardarelli, E., Pietrodangelo, A., Strincone, M., 2006. Determination of metals, metalloids and non-volatile ions in airborne particulate matter by a new two-step sequential leaching procedure: Part B: Validation on equivalent real samples. Talanta 69 (3), 588–595.
Carlberg, I., Mannervik, B., 1985. Glutathione Reductase. Methods in Enzymology 113, 484–490. https://doi.org/10.1016/S0076-6879(85)13062-4.
Chainy, G.B.N., Paital, B., Dandapat, J., 2016. An overview of seasonal changes in oxidative stress and antioxidant defence parameters in some invertebrate and vertebrate species. Scientifica 2016 (1), 6126570.
Charkiewicz, A.E., Omeljaniuk, W.J., Nowak, K., Garley, M., Nikliński, J., 2023. Cadmium toxicity and health effects—a brief summary. Molecules 28 (18), 6620.
Chen, L.C., Lippmann, M., 2009. Effects of metals within ambient air particulate matter (PM) on human health. Inhal. Toxicol. 21 (1), 1–31.
Chen, H., Oliver, B.G., Pant, A., Olivera, A., Poronnik, P., Pollock, C.A., Saad, S., 2022. Effects of air pollution on human health–mechanistic evidence suggested by *in vitro* and *in vivo* modelling. Environ. Res. 212, 113378.
Chianese, E., Galletti, A., Giunta, G., Landi, T.C., Marcellino, L., Montella, R., Riccio, A., 2018. Spatiotemporally resolved ambient particulate matter concentration by fusing observational data and ensemble chemical transport model simulations. Ecol. Model. 385, 173–181.
Chianese, E., Tirimberio, G., Riccio, A., 2019. $PM_{2.5}$ and PM_{10} in the urban area of Naples: chemical composition, chemical properties and influence of air masses origin. J. Atmos. Chem. 76, 151–169.
Chianese, E., Tirimberio, G., Appolloni, L., Dinoi, A., Contini, D., Di Gilio, A., Riccio, A., 2022. Chemical characterisation of PM 10 from ship emissions: A study on samples from hydrofoil exhaust stacks. Environ. Sci. Pollut. Res. 1–14.
Colombo, C., Monhemius, A.J., Plant, J.A., 2008. Platinum, palladium and rhodium release from vehicle exhaust catalysts and road dust exposed to simulated lung fluids. Ecotoxicol. Environ. Saf. 71, 722–730.
Council of European Union (2024). Directive 2024/2881 of the European Parliament and of the Council of 23 October 2024 on ambient air quality and cleaner air for Europe. URL ⟨https://eur-lex.europa.eu/eli/dir/2024/2881/oj⟩.
da Silva, L.I.D., Yokoyama, L., Maia, L.B., Monteiro, M.I.C., Pontes, F.V.M., Carneiro, M. C., Neto, A.A., 2015. Evaluation of bioaccessible heavy metal fractions in PM_{10} from the metropolitan region of Rio de Janeiro city, Brazil, using a simulated lung fluid. Microchem. J. 118, 266–271.
Dahl, J.U., Gray, M.J., Jakob, U., 2015. Protein quality control under oxidative stress conditions. J. Mol. Biol. 427 (7), 1549–1563.
Dinoi, A., Cesari, D., Marinoni, A., Bonasoni, P., Riccio, A., Chianese, E., Contini, D., 2017a. Inter-comparison of carbon content in $PM_{2.5}$ and PM_{10} collected at five measurement sites in Southern Italy. Atmosphere 8 (12), 243.
Dinoi, A., Donateo, A., Belosi, F., Conte, M., Contini, D., 2017b. Comparison of atmospheric particle concentration measurements using different optical detectors: Potentiality and limits for air quality applications. Measurement 106, 274–282.
Driver, A.S., Kodavanti, P.R.S., Mundy, W.R., 2000. Age-related changes in reactive oxygen species production in rat brain homogenates. Neurotoxicology Teratol. 22 (2), 175–181.
Duffò, G.S., Castillo, E.Q., 2004. Development of an artificial saliva solution for studying the corrosion behavior of dental alloys. Corrosion 60 (6), 594–602.
Ercal, N., Gurer-Orhan, H., Aykin-Burns, N., 2001. Toxic metals and oxidative stress part I: mechanisms involved in metal-induced oxidative damage. Curr. Top. Med. Chem. 1 (6), 529–539.
EzhilKumar, M.R., Karthikeyan, S., Chianese, E., Tirimberio, G., Di Gilio, A., Palmisani, J., Riccio, A., 2021. Vertical transport of PM2.5 and PM10 and its source identification in the street canyons of Chennai metropolitan city, India. Atmos. Pollut. Res. 12 (1), 173–183.
Foster, M., Samman, S., 2010. Zinc and redox signaling: perturbations associated with cardiovascular disease and diabetes mellitus. Antioxid. Redox Signal. 13 (10), 1549–1573.
Halliwell, B., Gutteridge, J.M., 1990. Role of free radicals and catalytic metal ions in human disease: an overview. Methods Enzymol. 186, 1–85.
Hamidi, M.R., Jovanova, B., Kadifkova Panovska, T., 2014. Toxicological evaluation of the plant products using Brine Shrimp (Artemia salina L.) model. Maced. Pharm. Bull. 60 (1), 9–18, 2014.
Heath, R.L., Tappel, A.L., 1976. A new sensitive assay for the measurement of hydroperoxides. Anal. Biochem. 76 (1), 184–191.
Huang, X., Betha, R., Tan, L.Y., Balasubramanian, R., 2016. Risk assessment of bioaccessible trace elements in smoke haze aerosols versus urban aerosols using simulated lung fluids. Atmos. Environ. 125, 505–511.
Innes, E., Yiu, H.H., McLean, P., Brown, W., Boyles, M., 2021. Simulated biological fluids–a systematic review of their biological relevance and use in relation to inhalation toxicology of particles and fibres. Crit. Rev. Toxicol. 51 (3), 217–248.
Jung, K.H., Torrone, D., Lovinsky-Desir, S., Perzanowski, M., Bautista, J., Jezioro, J.R., Miller, R.L., 2017. Short-term exposure to $PM_{2.5}$ and vanadium and changes in asthma gene DNA methylation and lung function decrements among urban children. Respir. Res. 18, 1–11.
Kanakidou, M., Mihalopoulos, N., Kindap, T., Im, U., Vrekoussis, M., Gerasopoulos, E., Moubasher, H., 2011. Megacities as hot spots of air pollution in the East Mediterranean. Atmos. Environ. 45 (6), 1223–1235.
Kastury, F., Smith, E., Juhasz, A.L., 2017. A critical review of approaches and limitations of inhalation bioavailability and bioaccessibility of metal (loid) s from ambient particulate matter or dust. Sci. Total Environ. 574, 1054–1074.
Kehrer, J.P., Klotz, L.O., 2015. Free radicals and related reactive species as mediators of tissue injury and disease: implications for health. Crit. Rev. Toxicol. 45 (9), 765–798.
Khansari, N., Shakiba, Y., Mahmoudi, M., 2009. Chronic inflammation and oxidative stress as a major cause of age-related diseases and cancer. Recent Pat. Inflamm. Allergy Drug Discov. 3 (1), 73–80.
Kim, K.H., Kabir, E., Kabir, S., 2015. A review on the human health impact of airborne particulate matter. Environ. Int. 74, 136–143.
Leclercq, B., Alleman, L.Y., Perdrix, E., Riffault, V., Happillon, M., Strecker, A., Coddeville, P., 2017. Particulate metal bioaccessibility in physiological fluids and cell culture media: toxicological perspectives. Environ. Res. 156, 148–157.
Li, Y.G., Gao, X., 2014. Epidemiologic studies of particulate matter and lung cancer. Chin. J. Cancer 33 (8), 376–380. https://doi.org/10.5732/cjc.014.10063.
Li, N., Kim, S., Wang, M., Froines, J., Sioutas, C., Nel, A., 2002. Use of a stratified oxidative stress model to study the biological effects of ambient concentrated and diesel exhaust particulate matter. Inhal. Toxicol. 14 (5), 459–486.
Li, Y., Kuppusamy, P., Zweier, J.L., Trush, M.A., 1995. ESR evidence for the generation of reactive oxygen species from the copper-mediated oxidation of the benzene metabolite, hydroquinone: role in DNA damage. Chem. Biol. Interact. 94 (2), 101–120.
Li, J., Song, H., Zhang, L., Li, J., Yang, Y., Cui, X., Tian, S., 2024. Interaction of diesel exhaust particulate matter with mucins in simulated saliva fluids: Bioaccessibility of heavy metals and potential health risks. J. Hazard. Mater. 480, 135811.
Li, H., Wu, H., Wang, Q.G., Yang, M., Li, F., Sun, Y., Wang, C., 2017. Chemical partitioning of fine particle-bound metals on haze–fog and non-haze–fog days in Nanjing, China and its contribution to human health risks. Atmos. Res. 183, 142–150.
Liochev, S.I., 2018. The mechanism of "Fenton-like" reactions and their importance for biological systems. A biologist's view. Met. ions Biol. Syst. 1–39.
Mariani, E., Mangialasche, F., Feliziani, F.T., Cecchetti, R., Malavolta, M., Bastiani, P., Mecocci, P., 2008. Effects of zinc supplementation on antioxidant enzyme activities in healthy old subjects. Exp. Gerontol. 43 (5), 445–451.
Marques, M.R., Loebenberg, R., Almukainzi, M., 2011. Simulated biological fluids with possible application in dissolution testing. Dissolution Technol. 18 (3), 15–28.
Mesquita, C.S., Oliveira, R., Bento, F., Geraldo, D., Rodrigues, J.V., Marcos, J.C., 2014. Simplified 2, 4-dinitrophenylhydrazine spectrophotometric assay for quantification of carbonyls in oxidized proteins. Anal. Biochem. 458, 69–71.
Moreno, T., Pérez, N., Querol, X., Amato, F., Alastuey, A., Bhatia, R., Gibbons, W., 2010. Physicochemical variations in atmospheric aerosols recorded at sea onboard the Atlantic–Mediterranean 2008 Scholar Ship cruise (Part II): Natural versus anthropogenic influences revealed by PM_{10} trace element geochemistry. Atmos. Environ. 44 (21-22), 2563–2576.
Motta, C.M., Simoniello, P., Arena, C., Capriello, T., Panzuto, R., Vitale, E., Ferrandino, I., 2019. Effects of four food dyes on development of three model species, Cucumis sativus, *Artemia salina* and *Danio rerio*: Assessment of potential risk for the environment. Environ. Pollut. 253, 1126–1135.
Mukhtar, A., Limbeck, A., 2013. Recent developments in assessment of bio-accessible trace metal fractions in airborne particulate matter: A review. Anal. Chim. Acta 774, 11–25.
Muruganandam, N., Mahalingam, S., Narayanan, R., Rajadurai, E., 2023. Meandered and muddled: a systematic review on the impact of air pollution on ocular health. Environ. Sci. Pollut. Res. 30 (24), 64872–64890.
Mylonas, C., Kouretas, D., 1999. Lipid peroxidation and tissue damage. Vivo 13 (3), 295–309.
Napolitano, G., Fasciolo, G., Venditti, P., 2021. Mitochondrial Management of Reactive Oxygen Species. Antioxid. (Basel) 10 (11), 1824. https://doi.org/10.3390/antiox10111824. PMID: 34829696; PMCID: PMC8614740.
Napolitano, G., Fasciolo, G., Venditti, P., 2022. The Ambiguous Aspects of Oxygen. Oxygen 2 (3), 382–409. https://doi.org/10.3390/oxygen2030027.
Napolitano, G., Fasciolo, G., Di Meo, S., Venditti, P., 2019. Vitamin E supplementation and mitochondria in experimental and functional hyperthyroidism: a mini-review. Nutrients 11 (12), 2900.
Nemmar, A., Hoylaerts, M.F., Hoet, P.H., Nemery, B., 2004. Possible mechanisms of the cardiovascular effects of inhaled particles: systemic translocation and prothrombotic effects. Toxicol. Lett. 149 (1-3), 243–253.
Ntungwe, N.E., Domínguez-Martín, E.M., Roberto, A., Tavares, J., Isca, V.M.S., Pereira, P., Cebola, M.J., Rijo, P., 2020. Artemia species: An Important Tool to Screen General Toxicity Samples. Curr. Pharm. Des. 26 (24), 2892–2908.
Pelucchi, C., Negri, E., Gallus, S., 2009. Long-term particulate matter exposure and mortality: a review of European epidemiological studies. BMC Public Health 9 (453).
Peters, A., 2005. Particulate matter and heart disease: Evidence from epidemiological studies. Toxicol. Appl. Pharmacol. 207 (2-1), 477–482.
Pham-Huy, L.A., He, H., Pham-Huy, C., 2008. Free radicals, antioxidants in disease and health. International Journal Biomedical Science IJBS 4 (2), 89.
Poirot, R.L., Wishinski, P.R., 1986. Visibility, sulfate and air mass history associated with the summertime aerosol in northern Vermont. Atmos. Environ. (1967) 20 (7), 1457–1469.

Popoola, L.T., Adebanjo, S.A., Adeoye, B.K., 2018. Assessment of atmospheric particulate matter and heavy metals: a critical review. Int. J. Environ. Sci. Technol. 15, 935–948.

Powell, S.R., 2000. The antioxidant properties of zinc. J Nutr. 130 (5S Suppl), 1447S–1454s. https://doi.org/10.1093/jn/130.5.1447S. PMID: 10801958.

Rajabi, S., Ramazani, A., Hamidi, M., Naji, T., 2015. *Artemia salina* as a model organism in toxicity assessment of nanoparticles. DARU J. Pharm. Sci. 23, 1–6.

Ren, H., Yu, Y., An, T., 2020. Bioaccessibilities of metal(loid)s and organic contaminants in particulates measured in simulated human lung fluids: A critical review. Environ. Pollut. 265, 115070.

Riccio, A., Barone, G., Chianese, E., Giunta, G., 2006. A hierarchical Bayesian approach to the spatio-temporal modeling of air quality data. Atmos. Environ. 40 (3), 554–566.

Riccio, A., Chianese, E., Agrillo, G., Esposito, C., Ferrara, L., Tirimberio, G., 2014. Source apportion of atmospheric particulate matter: a joint Eulerian/Lagrangian approach. Environ. Sci. Pollut. Res. 21 (23), 13160–13168.

Riccio, A., Chianese, E., Monaco, D., Costagliola, M.A., Perretta, G., Prati, M.V., Magliulo, V., 2016. Real-world automotive particulate matter and PAH emission factors and profile concentrations: Results from an urban tunnel experiment in Naples, Italy. Atmos. Environ. 141, 379–387.

Riccio, A., Chianese, E., Tirimberio, G., Prati, M.V., 2017. Emission factors of inorganic ions from road traffic: A case study from the city of Naples (Italy). Transp. Res. Part D Transp. Environ. 54, 239–249.

Rodríguez, S., Querol, X., Alastuey, A., de la Rosa, J., 2007. Atmospheric particulate matter and air quality in the Mediterranean: a review. Environ. Chem. Lett. 5, 1–7.

Roig, N., Sierra, J., Roviar, J., Schuhmacher, M., Dominigo, J.L., Nadal, M., 2013. *In vitro* tests to assess toxic effects of airborne PM_{10} samples. Correlation with metals and chlorinated dioxin and furans. Sci. Total Environ. 443, 791–797.

Sharma, P., Jha, A.B., Dubey, R.S., Pessarakli, M., 2012. Reactive oxygen species, oxidative damage, and antioxidative defense mechanism in plants under stressful conditions. J. Bot. 2012 (1), 217037.

Shi, H., Shi, X., Liu, K.J., 2004. Oxidative mechanism of arsenic toxicity and carcinogenesis. Jan Mol Cell Biochem. 255 (1-2), 67–78. https://doi.org/10.1023/b:mcbi.0000007262.26044.e8. PMID: 14971647.

Sies, H., 2018. On the history of oxidative stress: Concept and some aspects of current development. Curr. Opin. Toxicol. 7, 122–126.

Sousa, G., Azevedo, R., Almeida, A., Delerue-Matos, C., Wang, X., Rodrigues, F., Oliveira, M., 2023. Characterization of Metal Content in the Saliva of Firefighters: A Preliminary Study. In Occupational and Environmental Safety and Health V. Springer Nature Switzerland, Cham, pp. 305–315.

Squadrito, G.L., Cueto, R., Dellinger, B., Pryor, W.A., 2001. Quinoid redox cycling as a mechanism for sustained free radical generation by inhaled airborne particulate matter. Free Radic. Biol. Med. 31 (9), 1132–1138.

Stein, A.F., Draxler, R.R., Rolph, G.D., Stunder, B.J.B., Cohen, M.D., Ngan, F., Ngan, F., 2015. NOAA's HYSPLIT atmospheric transport and dispersion modeling system. Bull. Am. Meteorol. Soc. 96, 2059–2077.

Stopford, W., Turner, J., Cappellini, D., Brock, T., 2003. Bioaccessibility testing of cobalt compounds. J. Environ. Monit. 5 (4), 675–680.

Tomajoli, M.T.M., Di Donato, P., Della Corte, V., Covone, G., Fasciolo, G., Geremia, E., Napolitano, G., 2025. The brine shrimp Artemia franciscana as a model for astrobiological studies: Physiological adaptations to Mars-like atmospheric pressure conditions. Comparative Biochemistry Physiology Part A Molecular Integrative Physiology, 111825.

Valavanidis, A., Fiotakis, K., Vlachogianni, T., 2008. Airborne particulate matter and human health: toxicological assessment and importance of size and composition of particles for oxidative damage and carcinogenic mechanisms. J. Environ. Sci. Health Part C. 26 (4), 339–362.

Valavanidis, A., Fiotakis, K., Bakeas, E., Vlahogianni, T., 2005. Electron paramagnetic resonance study of the generation of reactive oxygen species catalysed by transition metals and quinoid redox cycling by inhalable ambient particulate matter. Redox Rep. 10 (1), 37–51.

Vanhaecke, P., Persoone, G., Claus, C., Sorgeloos, P., 1981. Proposal for a short-term toxicity test with Artemia nauplii. Ecotoxicol. Environ. Saf. 5 (3), 382–387.

Viana, M., Amato, F., Alastuey, A., Querol, X., Moreno, T., Garcia Dos Santos, S., Fernández-Patier, R., 2009. Chemical tracers of particulate emissions from commercial shipping. Environ. Sci. Technol. 43 (19), 7472–7477.

Waisberg, M., Joseph, P., Hale, B., Beyersmann, D., 2003. Molecular and cellular mechanisms of cadmium carcinogenesis. Toxicology 192, 95–117.

Wätjen, W., Beyersmann, D., 2004. Cadmium-induced apoptosis in C6 glioma cells: influence of oxidative stress. Biometals 17, 65–78.

Wiseman, C.L., 2015. Analytical methods for assessing metal bioaccessibility in airborne particulate matter: a scoping review. Anal. Chim. Acta 877, 9–18.

Wiseman, C.L., Zereini, F., 2014. Characterizing metal(loid) solubility in airborne PM_{10}, $PM_{2.5}$ and PM_1 in Frankfurt, Germany using simulated lung fluids. Atmos. Environ. 89, 282–289.

Wu, X., Cobbina, S.J., Mao, G., Xu, H., Zhang, Z., Yang, L., 2016. A review of toxicity and mechanisms of individual and mixtures of heavy metals in the environment. Environ. Sci. Pollut. Res. 23, 8244–8259.